Rapid Communications

Fluctuation-induced forces in driven systems with a diffusivity anomaly

Mauro Sellitto

Dipartimento di Ingegneria, Università degli Studi della Campania "Luigi Vanvitelli," Via Roma 29, 81031 Aversa, Italy and Abdus Salam International Centre for Theoretical Physics, Strada Costiera 11, 34151 Trieste, Italy

(Received 14 September 2020; accepted 26 October 2020; published 16 November 2020)

We show that Casimir-like forces in boundary-driven systems with a bulk diffusivity anomaly are enhanced by cooperative dynamical effects and can be made locally attractive or repulsive depending on the boundary densities. Theoretical predictions based on mean-field arguments and the explicit evaluation of the Casimir force in the fluctuating hydrodynamics framework are supported by Monte Carlo simulation of a two-dimensional ($2D$) exclusion process with selective kinetic constraints. Consistent with the entropic interpretation of the Casimir effect, we find that local repulsive forces do appear whenever finite-size transverse density fluctuations exceed their infinite-size value. Our results suggest that the bulk diffusivity anomaly is a crucial ingredient in the small-scale design of driven soft-matter systems with tunable fluctuation-induced forces.

DOI: 10.1103/PhysRevE.102.050101

Thermal equilibrium is inherently stable [1], yet systems in reciprocal equilibrium are not equivalent under a microscope: The latent molecular agitation at the bottom can be utterly different. This is best epitomized by kinetic constraints [2,3]: local time-reversible restrictions on the microscopic dynamical evolution of a system. They can slow down and possibly prevent thermalization, both in the classical [4] and quantum domains [5]. But, paradoxically enough, the nondissipative dynamical activity that kinetic constraints generate becomes especially relevant in the presence of a dissipative mechanism, e.g., when a system is brought out of equilibrium by non-Hamiltonian forces [6,7]. To emphasize its importance, the term "frenesy" [8] was introduced in analogy with the role entropy plays in equilibrium. A most striking manifestation occurs in driven diffusive systems where the Casimir-like force arising from long-range nonequilibrium fluctuations [9] acquires a frenetic contribution that can change its sign and magnitude [10]. This feature can be relevant in the small-scale design of soft-matter systems and devices [11]. However, finding physical systems in which it can be actually observed, measured, and properly quantified is hard.

In this paper, we make a step forward in this direction by showing that systems with a diffusivity anomaly when driven in a nonequilibrium steady state by two boundary particle reservoirs display enhanced fluctuation-induced force (FIF), which can be locally attractive or repulsive depending on the distance from the reservoirs and on their densities. We first consider a microscopic realization of a system with a diffusivity anomaly [12] and show how to get an accurate estimation of FIF by exploiting only a sufficiently precise knowledge of the steady-state density profile, no matter the underlying dynamics. The calculation is an improvement over a mean-field approach [13] and agrees remarkably well with the direct measurement of FIF we present here using a recently devised Monte Carlo algorithm [14]. Finally, we show that locally repulsive FIF do emerge whenever finite-size transverse density fluctuations are larger than their infinite-size limiting value. This is consistent with the entropic interpretation of the Casimir effect [9] and offers a convenient alternative diagnostic tool possibly useful in numerics and experiments, e.g., on driven colloids.

We consider a two-dimensional driven diffusive system, with local particle density $\rho(\mathbf{x}, t)$ at position $\mathbf{x} = (x, y)$ and time t, obeying the conservation equation

$$\partial_t \rho + \partial_x J = 0, \tag{1}$$

where the stochastic particle current J is

$$J = -D(\rho)\, \partial_x \rho + \eta(x, t). \tag{2}$$

Here, $D(\rho)$ is a density-dependent diffusion coefficient and $\eta(\mathbf{x}, t)$ is a space-time uncorrelated white noise with zero mean and variance satisfying a fluctuation-dissipation condition $\sigma(\rho) = 2\,\rho^2\, D(\rho)\,\kappa(\rho)$, where $\kappa(\rho)$ is the fluid compressibility and we set the prefactor $k_{\mathrm{B}}T = 1$ throughout. The density is subject to the boundary condition $\rho(0, y, t) = \rho_0$ and $\rho(L, y, t) = \rho_1$ for any y, t (see Fig. 1 for an illustration of the setup). Within the framework of fluctuating hydrodynamics, it has been predicted in Ref. [10] that the fluctuation-induced pressure $\Pi(x)$ between two parallel slabs at distance ℓ is, to the leading order in $\delta\rho = \rho_1 - \rho_0$, given by

$$\Pi(x) = \frac{(\delta\rho)^2}{4L\ell}\, P''|_{\overline{\rho}(x)}\, c(x), \tag{3}$$

where P is the pressure, the prime denotes the derivative with respect to the particle density, and $c(x)$ is a nonequilibrium correlation factor:

$$c(x) = \left[\left(\frac{\rho}{P'}\right)'' + \left(\frac{\rho}{P'}\frac{D'}{D}\right)'\right]\frac{x}{L}\left(1 - \frac{x}{L}\right). \tag{4}$$

Equation (4) is counterintuitive because one would naively expect that Π depends only upon the thermodynamic state variables, while it contains a term that explicitly depends on

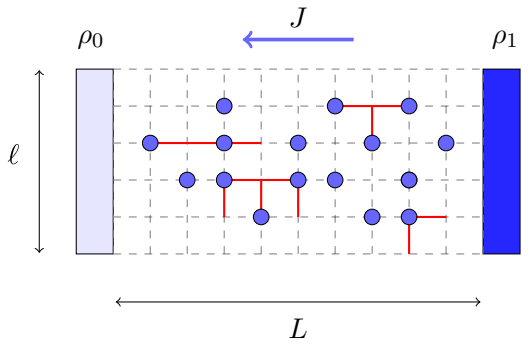

FIG. 1. The setup considered in Monte Carlo simulations consists of a square lattice of size $\ell \times L$ connected to two reservoirs at $x = 0$ and $x = L$, with densities $\rho(0, y) = \rho_0$ and $\rho(L, y) = \rho_1 > \rho_0$, respectively. There are periodic boundary conditions in the direction transverse to the particle flux J. The bulk dynamics is governed by a selective kinetic constraint obeying the detailed balance condition: A particle can hop to a nearby empty site only if it is not surrounded by two nearest neighboring particles before and after the move. Red bonds show forbidden hoppings due to the selective kinetic constraint on a specific configuration of particles. (Hoppings forbidden by the pure hard-core exclusion are not shown.)

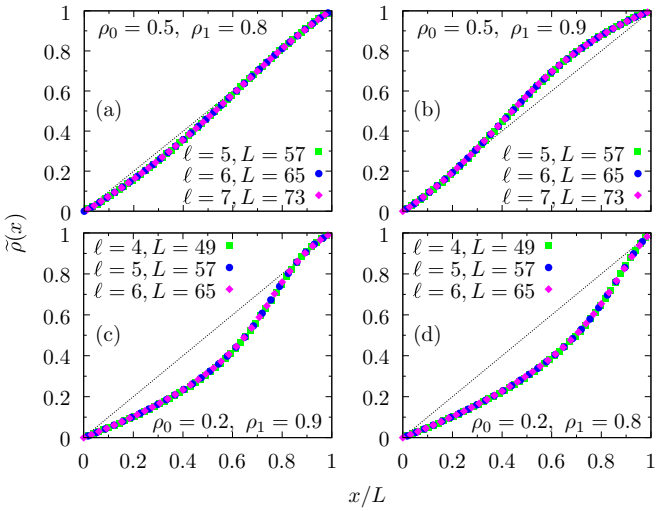

FIG. 2. Normalized profiles, $\widetilde{\rho}(x) = [\rho(x) - \rho_0]/(\rho_1 - \rho_0)$, in the cooperative exclusion process with selective kinetic constraints on a square lattice of size $L \times \ell$. The system edges at $x = 0$ and $x = L$ are in contact with a particle reservoir at density ρ_0 and ρ_1, respectively. There are periodic boundary conditions in the direction transverse to the particle current. For comparison, the density profile for the simple exclusion process is shown as a dotted straight line.

the diffusion coefficient. This purely dynamic or "frenetic" contribution is very important because it can turn FIF from attractive to repulsive, when $D(\rho)$ presents a minimum at a certain density. However, its physical relevance is unclear and was left widely open in Ref. [10], where FIF predictions were tested only in a very simple case, namely, the simple symmetric exclusion process, for which $D(\rho) = 1$. In fact, two stumbling blocks prevent the direct evaluation of Eqs. (3) and (4): The equation of state and the bulk diffusion coefficient are hardly known exactly, even for schematic model systems.

To get around these difficulties, we consider a stochastic lattice gas that can be viewed as a coarse-grained schematic description of a complex fluid in which molecular motion is hindered by steric effects when the local environment is neither densely packed nor too loose. Microscopically, this condition can be implemented on a square lattice by imposing that a particle can move to a nearby empty site if and only if the particle does not possess two particles as nearest neighbors, before and after the move [12]. This selective kinetic constraint requires (weakly) cooperative rearrangements of particles only in an intermediate range of density, while it becomes ineffective when density is either small or large (and the simple exclusion process is recovered). In this way, the model becomes endowed with a density minimum in the bulk diffusion, which we call the (bulk) diffusivity anomaly, in analogy with the (self-)diffusivity anomaly that has been especially studied in water [15,16] and other systems [17,18].

The selective kinetic constraint obeys the detailed balance condition and the associated Markov chain is irreducible over the whole configuration space [12]. Therefore, the system thermodynamics is trivial and the equation of state is

$$P(\rho) = -\ln(1 - \rho)\,, \tag{5}$$

which significantly simplifies the evaluation of Eq. (4). It is important to contrast the selective kinetic constraint considered here with those used to model glassy behaviour [2,3]. The *equilibrium* dynamics is highly nontrivial in the latter [19], while in the former it is pretty unremarkable [12]. However, unexpected features, such as highly nontrivial convexity-change density profiles, are brought to life in a nonequilibrium steady state. Figure 2 shows the absence of finite-size effect in the density profiles obtained in Monte Carlo simulations for system sizes and densities of boundary reservoirs, for which the FIF dynamical contribution will be assessed later on. Interestingly, profile convexity can be predicted within a no-correlation approximation for the diffusion coefficient [12]:

$$D_{\text{NCA}}(\rho) = [1 - 3\rho^2(1 - \rho)]^2\,, \tag{6}$$

which can be easily interpreted as the probability for particle hopping to a nearby empty site, with the term $3\rho^2(1 - \rho)$ encoding the selective kinetic constraint on the departure and arrival site under the assumption that occupation variables are uncorrelated (the power 2 on square brackets accounting for the microscopic time reversibility, i.e., the detailed balance condition). Although crude, such a mean-field approach provides a useful guide in estimating the density minimum in the diffusion coefficient ($\rho^\star = 2/3$) and, therefore, the region of parameter space in which repulsive FIF can be observed [13]. Unfortunately, going beyond the no-correlation approximation is challenging for nongradient systems such as those considered here [20,21]. For this reason, we follow an alternative route allowing the evaluation of FIF in a generic athermal system, even in the absence of any information about $D(\rho)$. In fact, by observing that the dynamical contribution enters Eq. (4) only through the ratio of the diffusion coefficient and its derivatives, we exploit the knowledge of the steady-state

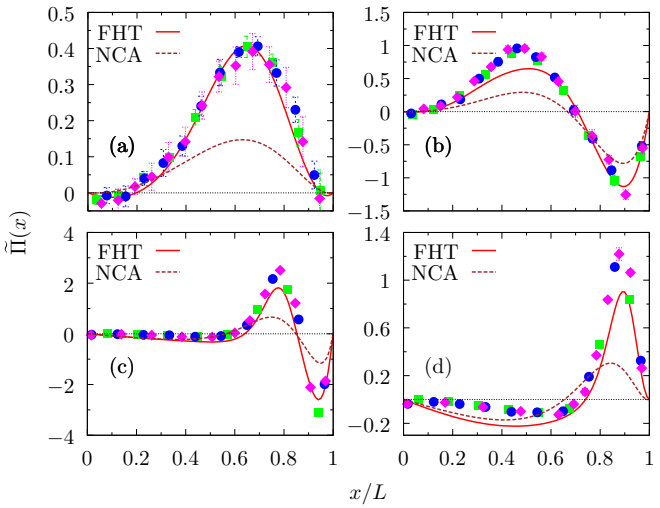

FIG. 3. Main paper results: Rescaled fluctuation-induced pressure $\widetilde{\Pi}(x) = \ell L \Pi(x)$ in a cooperative exclusion process with selective kinetic constraint on a square lattice. Dashed lines are the predictions based on the no-correlation approximation (NCA) of bulk diffusion. Full lines are the predictions of fluctuating hydrodynamics theory (FHT) obtained from estimating density profiles with a fifth- or sixth-order polynomial. Data points refer to the direct measurement of pressure by Monte Carlo (MC) simulations of 10^8 MC sweeps (average over 10 independent realizations): multiple ghost sites with volume $\Delta V = 2\,\ell$, $\lambda \in [0, 1]$ discretized into 24 values equally spaced over three contiguous subintervals ([0.01,0.04], [0.04,0.2], and [0.2,1], with a cutoff $\lambda_{\min} = 0.001$). Panel parameters for system sizes and boundary densities as in Fig. 2. Statistical errors on data points are only visible in panel (a) because of the lower signal-to-noise ratio.

inverse density profile $x(\rho)$,

$$x(\rho) = a + b \int D(\rho) d\rho \,, \tag{7}$$

where the constants a and b are fixed by the boundary condition $x(\rho_0) = 0$ and $x(\rho_1) = L$, to write

$$\frac{D'}{D} = \frac{x''}{x'} \tag{8}$$

and analogous relations for other derivative ratios. This identity enables us to express the dynamic contribution to Eq. (4) only in terms of ratios of $x(\rho)$ derivatives:

$$\left(\frac{\rho}{P'}\frac{D'}{D}\right)' = (1-2\rho)\frac{x''}{x'} + \rho(1-\rho)\left[\frac{x'''}{x'} - \left(\frac{x''}{x'}\right)^2\right]. \tag{9}$$

Therefore, even though the FIF certainly depends on the dynamics, it does so only through a specific dependence on the density profile, at least to the order $(\delta\rho)^2$. To make this shortcut even more concrete, we approximate the function $x(\rho)$ obtained in a Monte Carlo simulation with a low-order polynomial. This allows the evaluation of its derivatives without introducing extra numerical approximations. The predictions of fluctuating hydrodynamics, obtained with this procedure through Eq. (9), are illustrated in Fig. 3, where they are compared with those obtained with Eq. (6). We see that the FIF sign is consistently well reproduced, while the FIF magnitude is underestimated in the mean-field approach. This suggests that long-range dynamical fluctuations in the particle motion correlations are the main source of FIF enhancement. To understand the extent to which they are encoded in the density profile and to better assess the merit of the above procedure we need, however, an explicit direct evaluation of FIF.

The task of measuring directly the pressure of a systems of particles without kinetic energy on a lattice is not an easy one, especially in nonequilibrium conditions and in the presence of inhomogeneous density profiles. We exploit here a recently devised Monte Carlo algorithm [14] that takes advantage of the Dickman method [22]. We consider an auxiliary system in which multiple ghost sites of volume δV are added to the original system of volume V. Ghost sites play the role of pressure probes and are subject to a repulsive potential of magnitude $U_\lambda = -k_B T \ln \lambda$. Simple thermodynamic relations lead to express the system pressure as

$$P = \lim_{\delta V \to 0} \int_0^1 \langle \rho_{\Delta V} \rangle \frac{d\lambda}{\lambda} \,, \tag{10}$$

where $\langle \rho_{\Delta V} \rangle$ is the average fraction of particles in δV. For purely hard-core interactions, $\langle \rho_{\Delta V} \rangle$ is exactly determined in the infinite-size limit,

$$\langle \rho_{\Delta V} \rangle = \frac{\lambda \rho}{1 - \rho + \lambda \rho} \tag{11}$$

(as can be checked by direct integration). For inhomogeneous systems, the spatial dependence of density, $\rho = \rho(x)$, has to be included and therefore the FIF profile can be measured as

$$\Pi_{\rm MC}(x) \approx \int_0^1 \left[\langle \rho_{\Delta V}(x) \rangle - \frac{\lambda \rho(x)}{1 - \rho(x) + \lambda \rho(x)} \right] \frac{d\lambda}{\lambda} \,, \tag{12}$$

where it is understood that $\delta V \ll V$, and the integral is performed numerically by discretizing the interval [0,1]. Monte Carlo results for the two-dimensional cooperative exclusion process with selective kinetic constraint are shown in Fig. 3 as data points. We see that in an intermediate range of densities of boundary reservoirs FIF is repulsive and generally enhanced. The agreement with the fluctuating hydrodynamic predictions obtained with Eq. (9) is very good and, in some cases [Fig. 3(a)] excellent. A closer look at the peaks of the FIF estimated to the order $(\delta\rho)^2$ through Eq. (9), and the one measured through Monte Carlo simulation in Fig. 3, Eq. (12), shows that their difference increases with $\delta\rho$. This suggests that the origin of the observed discrepancies is due, at least in part, to the next-to-leading-order contributions to FIF. In general, however, the nonextensive scaling of $\Pi(x)$ predicted in Ref. [10] is confirmed, and the attractive FIF found in the simple exclusion process [10] is recovered when the local density is either small or large. It is interesting to notice the exquisite dependence of FIF upon the profile curvature: If the overall shape is very near to a straight line, as in Fig. 2(a), the resulting FIF turns out to be globally repulsive rather than attractive, as one would naively expect from the simple exclusion process. This means that some caution is required in guessing the FIF sign from $\rho(x)$.

Finally, we mention that an alternative signature of the rich features displayed by FIF can be observed in the spatial dependence of transverse density fluctuations. Although for

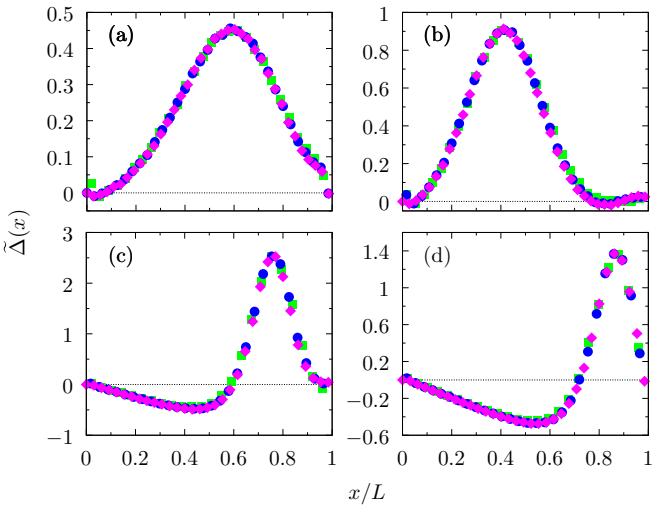

FIG. 4. Rescaled excess of transverse density fluctuations $\widetilde{\Delta}(x) = 100\,\Delta(x)\,(\ell \times L)^{1/4}$ for the cooperative exclusion process with selective kinetic constraint on a square lattice. The factor 100 is included for sake of a better comparison with Fig. 3. Panel parameters as in Fig. 2.

large system sizes they appear to be uncorrelated [12], a more careful finite-size analysis shows well-defined deviations from the equilibrium value. This is appreciated by plotting the excess of transverse density fluctuations $\Delta(x)$:

$$\Delta(x) = \ell[\langle\rho(x)^2\rangle - \langle\rho(x)\rangle^2] - \langle\rho(x)\rangle[1 - \langle\rho(x)\rangle]\,. \quad (13)$$

Figure 4 shows the rescaled excess $\widetilde{\Delta}(x) = \Delta(x)(\ell\,L)^{1/4}\,100$ for system parameters corresponding to Fig. 2 (and Fig. 3). The data collapse suggests that $\Delta(x)$ scales with system size as $(\ell\,L)^{-1/4}$ and, more importantly, that it does follow a pattern very similar to that observed for FIF, at corresponding values of system parameters, in Fig. 3. Similarly, in the simple symmetric exclusion process $\Delta(x)$ is always negative (and obeys the same finite-size scaling), concurrently with the universal attractive nature of FIF. This seems consistent with the entropic interpretation of the Casimir effect [9]. The enhancement of transverse fluctuations in the intermediate range of density around the diffusivity minimum can be intuitively interpreted as due to the extra cooperative rearrangements required by the selective kinetic constraint to sustain a steady-state particle current. Nevertheless, the behavior near the edge at $x = L$, in Figs. 4(b) and 4(c), where FIF changes rather quickly from repulsion to attraction, cannot be interpreted along this line of thought. We were not able to come up with a satisfactory explanation of this behavior and leave this puzzle to a future work.

In summary, we have investigated FIF in driven systems with a diffusivity anomaly by three independent methods. The direct Monte Carlo evaluation in a lattice model shows that FIF is generally enhanced and can be attractive as well as repulsive, depending on the densities of reservoirs. Our analysis confirms that a simple mean-field approach is an effective heuristic tool for predicting the FIF sign, even though it underestimates the FIF magnitude. We suggested how to extract more detailed quantitative predictions from the fluctuating hydrodynamic results to the order $(\delta\rho)^2$ [10], by taking the density profile as unique input. This method is general and can be applied to the numerical and experimental investigation of other systems, even in the absence of detailed information on bulk diffusion. It would be interesting, for example, to confirm the above findings in more realistic nearest-neighbor exclusion models. In fact, since FIF depends, to the leading order in $\delta\rho$, upon the density profile alone (the dependence on microscopic dynamics being generally mild), and pressure is a nondecreasing function of particle density (for local equilibrium states), we expect that Eqs. (3) and (4) will not be significantly affected, on a qualitative level, by the differences in the equation of state and bulk diffusion of the various models one can consider. Therefore, our results should be rather robust and broadly relevant to athermal system with a diffusivity anomaly in a quasi-isothermal environment. In particular, once the boundary densities are such that the density profile goes through the diffusivity minimum, one should observe a repulsive FIF. In the presence of a temperature gradient, however, the FIF contribution arising from the coupling between hydrodynamics modes will become dominant [23].

In conclusion, the generation of attractive and repulsive forces by means of nonequilibrium dynamical fluctuations at the microscopic scale is a remarkable example of the relevance of the bulk diffusivity anomaly and might play a role in a variety of cellular and biochemical (isothermal) processes in which mechanical forces of the order of pN are involved within the organism [24–26]. It could also offer opportunities for the design of micromechanical soft matter systems [11] and be experimentally accessible [27,28].

[1] H. B. Callen, *Thermodynamics and an Introduction to Thermostatistics* (J. Wiley & Sons, New York, 1985).
[2] G. H. Fredrickson and H. C. Andersen, Kinetic Ising Model of the Glass Transition, Phys. Rev. Lett. **53**, 1244 (1984).
[3] W. Kob and H. C. Andersen, Kinetic lattice-gas model of cage effects in high-density liquids and a test of mode-coupling theory of the ideal-glass transition, Phys. Rev. E **48**, 4364 (1993).
[4] F. Ritort and P. Sollich, Glassy dynamics of kinetically constrained models, Adv. Phys. **52**, 219 (2003).
[5] J. P. Garrahan, Aspects of non-equilibrium in classical and quantum systems: Slow relaxation and glasses, dynamical large deviations, quantum non-ergodicity, and open quantum dynamics, Phys. A (Amsterdam, Neth.) **504**, 130 (2018).
[6] R. Landauer, Statistical physics of machinery: Forgotten middle-ground, Phys. A (Amsterdam, Neth.) **194**, 551 (1993).
[7] M. Baiesi and C. Maes, Life efficiency does not always increase with the dissipation rate, J. Phys. Comm. **2**, 045017 (2018).
[8] C. Maes, Frenesy: Time-symmetric dynamical activity in nonequilibria, Phys. Rep. **850**, 1 (2020).
[9] M. Kardar and R. Golestanian, The "friction" of vacuum, and other fluctuation-induced forces, Rev. Mod. Phys. **71**, 1233 (1999).

[10] A. Aminov, Y. Kafri, and M. Kardar, Fluctuation-Induced Forces in Nonequilibrium Diffusive Dynamics, Phys. Rev. Lett. **114**, 230602 (2015).

[11] L. M. Woods, D. A. R. Dalvit, A. Tkatchenko, P. Rodriguez-Lopez, A. W. Rodriguez, and R. Podgornik, Materials perspective on Casimir and van der Waals interactions, Rev. Mod. Phys. **88**, 045003 (2016).

[12] M. Sellitto, Cooperative transport with selective kinetic constraints, Phys. Rev. E **100**, 040102(R) (2019).

[13] M. Sellitto, Casimir-like forces in cooperative exclusion processes, J. Phys. A: Math. Theor. **53**, 01LT01 (2020).

[14] M. Sellitto, Measuring pressure in equilibrium and nonequilibrium lattice-gas models, J. Chem. Phys. **153**, 161101 (2020).

[15] F. de los Santos and G. Franzese, Relations between the diffusion anomaly and cooperative rearranging regions in a hydrophobically nanoconfined water monolayer, Phys. Rev. E **85**, 010602(R) (2012).

[16] L. B. Krott and M. C. Barbosa, Anomalies in a waterlike model confined between plates, J. Chem. Phys. **138**, 084505 (2013).

[17] L. Berthier, A. J. Moreno, and G. Szamel, Increasing the density melts ultrasoft colloidal glasses, Phys. Rev. E **82**, 060501(R) (2010).

[18] M. Pica Ciamarra and P. Sollich, Dynamics and instantaneous normal modes in a liquid with density anomalies, J. Phys.: Condens. Mat. **27**, 194128 (2015).

[19] C. Toninelli, G. Biroli, and D. S. Fisher, Spatial Structures and Dynamics of Kinetically Constrained Models of Glasses, Phys. Rev. Lett. **92**, 185504 (2004).

[20] E. Teomy and Y. Shokef, Hydrodynamics in kinetically constrained lattice-gas models, Phys. Rev. E **95**, 022124 (2017).

[21] C. Arita, P. L. Krapivsky, and K. Mallick, Bulk diffusion in a kinetically constrained lattice gas, J. Phys. A: Math. Theor. **51**, 125002 (2018).

[22] R. Dickman, New simulation method for the equation of state of lattice chains, J. Chem. Phys. **87**, 2246 (1987).

[23] T. R. Kirkpatrick, J. M. Ortiz de Zárate, and J. V. Sengers, Physical origin of nonequilibrium fluctuation-induced forces in fluids, Phys. Rev E **93**, 012148 (2016).

[24] C. Bustamante, Y. R. Chemla, N. R. Forde, and D. Izhaky, Mechanical processes in biochemistry, Annu. Rev. Biochem. **73**, 705 (2004).

[25] P. Roca-Cusachs, V. Conte, and X. Trepat, Quantifying forces in cell biology, Nat. Cell Biol. **19**, 742 (2017).

[26] E. Hannezo and C.-P. Heisenberg, Mechanochemical feedback loops in development and disease, Cell **178**, 12 (2019).

[27] C. Hertlein, L. Helden, A. Gambassi, S. Dietrich, and C. Bechinger, Direct measurement of critical Casimir forces, Nature (London) **451**, 172 (2008).

[28] A. Magazzù, A. Callegari, J. P. Staforelli, A. Gambassi, S. Dietrich, and G. Volpe, Controlling the dynamics of colloidal particles by critical Casimir forces, Soft Matter **15**, 2152 (2019).